

Prediction of elevated temperature, creep and damping behaviour of composite laminates from quantitative DMTA

G. Kotsikos, A. M. Robinson and A. G. Gibson*

The Cole–Cole (C–C) and Havriliak–Negami models respectively, have been identified as suitable for the parametric modelling of time and temperature behaviour of composites with symmetrical and asymmetrical retardation time spectra. For C–C a shortcut method is proposed to enable the prediction of creep behaviour from dynamic mechanical and thermal analysis (DMTA) data. The C–C plot provides a method of characterising the retardation time distribution, independently of any time–temperature equivalence relationship. The isophthalic polyester resin and composites examined in the present study all showed symmetrical retardation time spectra (in log time) and their DMTA behaviour was well modelled using C–C, with the added assumption of Arrhenius relaxation kinetics. The proposed creep model also worked well for these materials.

Keywords: DMTA, Creep, Composites

List of symbols

$E, E^*(\omega), E(t)$	modulus, complex modulus, creep modulus
E_U, E_R	unrelaxed and relaxed modulus
E_{U_0}, k	unrelaxed modulus at 0°C, temperature coefficient
E', E''	storage modulus, loss modulus
H	activation energy
$J, J^*(\omega), J(t)$	compliance, complex compliance, creep compliance
J_U, J_R	unrelaxed and relaxed compliance
J', J''	storage compliance, loss compliance
R	Boltzmann's constant
t	time
T, T_R, T'	absolute temperature, K; absolute reference temperature, °C; temperature, °C
α	retardation time distribution broadening parameter
β	retardation time distribution asymmetry parameter
τ, τ_0	retardation time, principal retardation time
$\tan\delta$	mechanical loss factor
$\phi(\ln\tau)$	retardation time distribution
$\psi'(\omega), \psi''(\omega), \psi(t)$	DMTA storage and loss functions, creep function
ω	frequency

Introduction

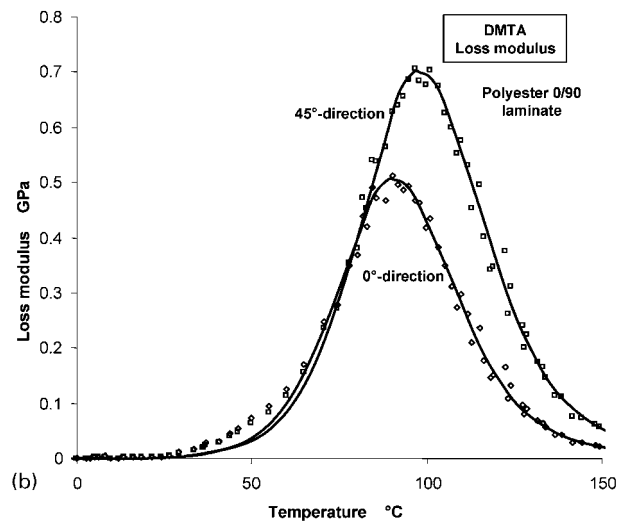
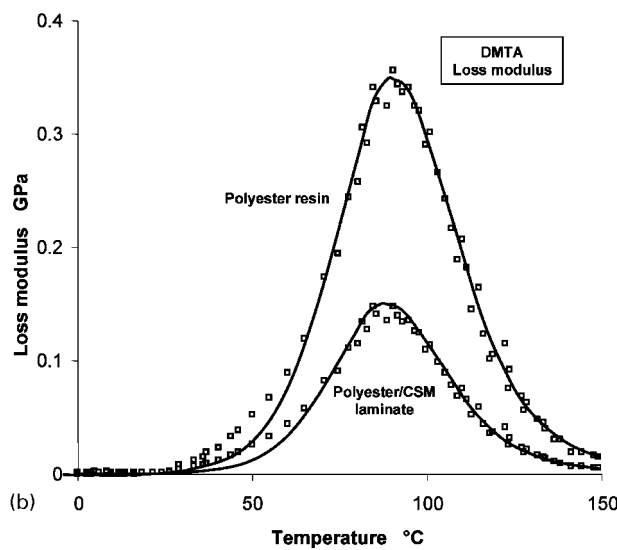
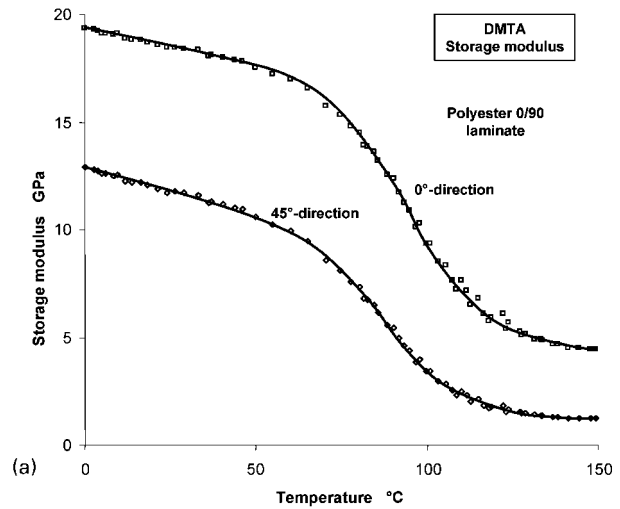
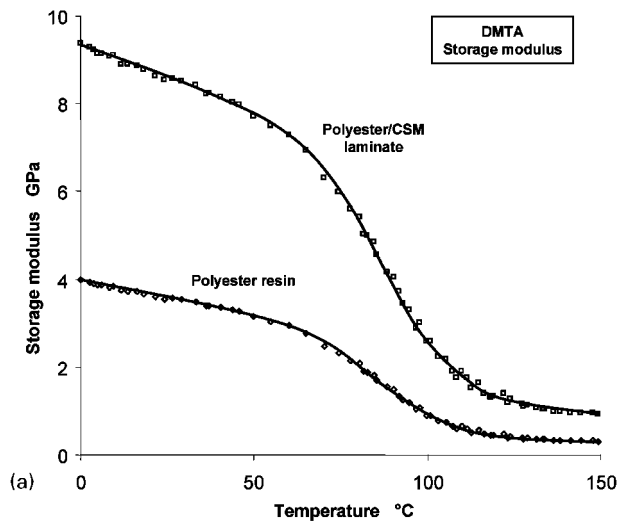
Dynamic mechanical and thermal analysis (DMTA) is commonly used as a semiquantitative technique for

characterising the properties of composites and assessing changes owing to processing, composition or environment.^{1–3} Although the technique is mainly used for comparison purposes, it can provide much more fundamental information relating to material relaxation behaviour. Ensuring accurate values for unrelaxed and relaxed moduli is important to facilitate the quantitative modelling of composite properties in the linear viscoelastic region. Laminate engineering properties, such as the creep modulus and the damping factor, which would otherwise be expensive to measure directly, can then be accurately predicted as a function of temperature. The present paper proposes a methodology for treating DMTA data, based on classical 1960's studies on dielectric behaviour.^{4–7} In cases where the retardation time distribution is symmetrical in log time the Cole–Cole (C–C) model⁴ may be modified for use with mechanical data. Havriliak and Negami^{5,6} later generalised this model to include non-symmetrical relaxation time distributions.

The DMTA behaviour of isophthalic polyester resin and glass polyester laminates was used to investigate the applicability of the procedure proposed to thermosetting resins and their composites. The materials chosen are widely used in marine composites. For these materials the retardation time spectra were found to be symmetrical in log time, allowing the C–C model to be employed. With the C–C model, it was found that creep behaviour in the linear viscoelastic region could be predicted using DMTA data. In addition, the effects of laminate ply structure could be modelled using complex versions of well known micromechanics expressions. This approach enables resin DMTA behaviour to be deduced from measurements on laminates, and *vice versa*.

University of Newcastle upon Tyne, UK

*Corresponding author, email a.g.gibson@ncl.ac.uk



a storage modulus; b loss modulus
 1 Data of DMTA (1 Hz and 10°C min⁻¹) for isophthalic polyester and for polyester CSM composite: continuous curves represent C-C model fits, with parameters shown in Table 1

a storage modulus; b loss modulus
 2 Data of DMTA (1 Hz and 10°C min⁻¹) for polyester/glass 0/90° laminate in 0 and 45° directions: continuous curves represent C-C model fits, with parameters shown in Table 1

Experimental

The DMTA curves were measured for pure isophthalic polyester resin and for 3 mm thick samples machined from chopped strand mat (CSM) and biaxial woven roving (WR) laminates, at 1 Hz, with a heating rate of 10°C min⁻¹, in the single cantilever beam bending mode. The as measured spectra were corrected for modelling purposes: storage moduli were adjusted to ensure that the unrelaxed and relaxed values agreed with accurate results obtained from the flexural creep measurements.

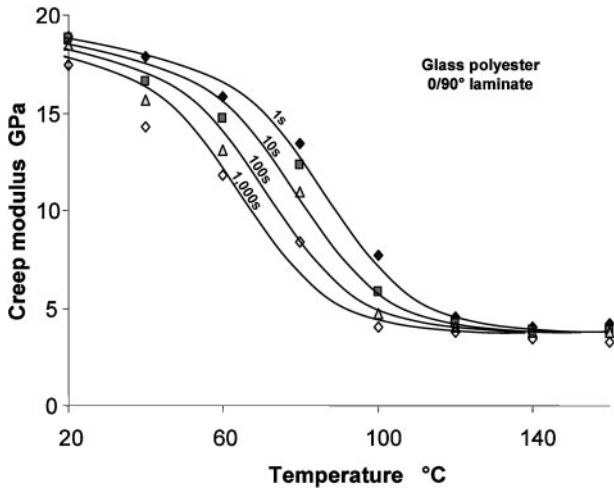
This was accomplished by making a linear adjustment to the log *E'* results. In addition, a background subtraction (linear in temperature) was made to the loss factor plot, to ensure zero tanδ at the upper and lower end of the temperature scale. The corrected DMTA results for the resin sample and CSM laminate are shown in Fig. 1, while those for the 0/90° laminate, in the 0 and 45° directions, are in Fig. 2.

A series of flexural creep measurements was also made, for the 0/90° laminate, in the 0° direction, to investigate the conversion of DMTA data to creep data, and to obtain accurate values of the unrelaxed and relaxed moduli. The results are shown in Fig. 3.

Table 1 Fitting parameters for materials investigated*

	Pure resin	CSM	WR (0/90°)	WR (±45°)
C-C parameter α	0.160	0.166	0.155	0.165
0°C unrelaxed modulus E_{U_0} , GPa	3.95	9.6	18.0	12.9
Thermal coefficient of E_{U_0} , GPa °C ⁻¹	0.015	0.02	0.02	0.02
Relaxed modulus E_R , GPa	0.29	0.87	4.20	1.14
Reference temperature T_R , °C	115	116	116	116

* In all cases it was assumed that activation energy, $H/R=34\ 000$ K, and the Havriliak-Negami (H-N) parameter, $\beta=1$.



3 Flexural creep modulus in 0° direction versus temperature for glass/polyester 0/90° laminate: continuous curves represent C–C model fit

Theory

Although the single relaxation time (SRT) model for time dependent behaviour is qualitatively useful in providing a framework for understanding relaxations, and appears in all the textbooks, it has very limited practical significance because real polymer relaxations are always much broader in temperature or frequency, because processes with more than one relaxation time are present. It is generally necessary to model this in terms of a multiplicity of Maxwell elements with different retardation times, as shown in Fig. 4. When a distribution of retardation times is present the complex compliance is given by the well known^{1–3} modification of Debye’s expression

$$J^*(\omega) = J_U + (J_R - J_U) \int_{-\infty}^{\infty} \frac{\phi(\ln \tau) d(\ln \tau)}{1 + i\omega\tau_i} \quad (1)$$

where the distribution function obeys the relationship

$$\int_{-\infty}^{\infty} \phi(\ln \tau) d(\ln \tau) = 1$$

so

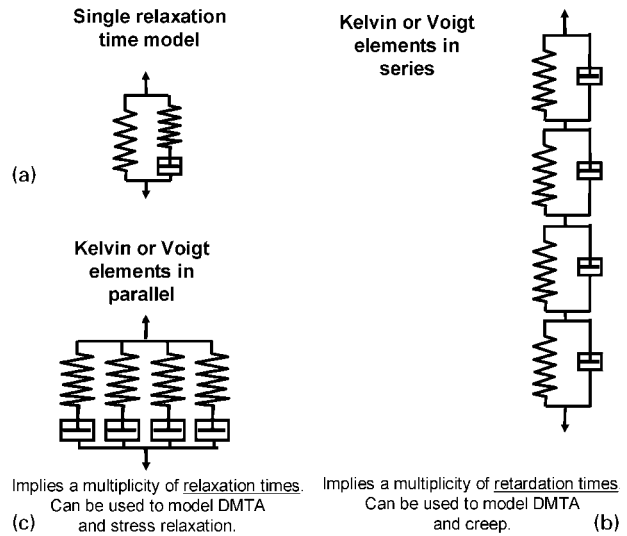
$$J'(\omega) = J_U + (J_R - J_U) \int_{-\infty}^{\infty} \frac{\phi(\ln \tau) d(\ln \tau)}{1 + \omega^2\tau^2} = J_U + (J_R - J_U)\psi'(\omega) \quad (2)$$

and

$$J''(\omega) = (J_R - J_U) \int_{-\infty}^{\infty} \frac{\phi(\ln \tau) \omega\tau d(\ln \tau)}{1 + \omega^2\tau^2} = (J_R - J_U)\psi''(\omega) \quad (3)$$

For the case of creep

$$J(t) = J_U + (J_R - J_U) \int_{-\infty}^{\infty} \phi(\ln \tau) (1 - e^{-t/\tau}) d(\ln \tau) = J_U + (J_R - J_U)\psi(t) \quad (4)$$



a single relaxation time model; b Maxwell elements in series, with multiple retardation times; c Maxwell elements in parallel, with multiple relaxation times

4 Models for linear viscoelastic behaviour

The functions $\psi'(\omega)$, $\psi''(\omega)$ and $\psi(t)$ are convenient abbreviations for the integral expressions. Retardation time distributions that are symmetrical when plotted as a function of $\ln \tau$ also produce symmetrical distributions of J' and ‘antisymmetrical’ distributions of J'' when plotted in log frequency space. However, there is no intrinsic reason why the retardation time spectrum for a particular material should be symmetrical and there are probably several polymer systems where this is not the case. It is useful, therefore, to consider a more general model capable of dealing with both the symmetrical and non-symmetrical cases.

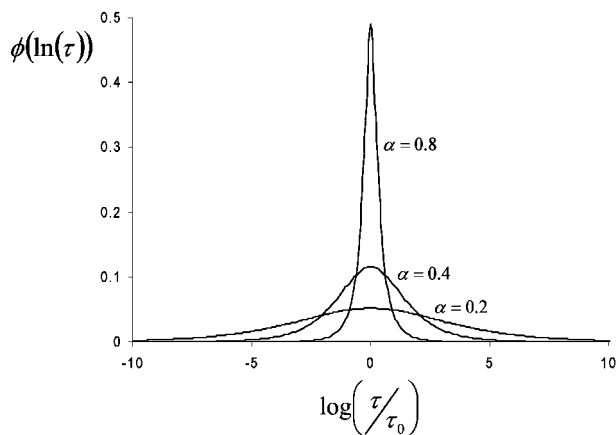
It is also relevant to note the significance of the area under the loss peak in frequency, namely that

$$\frac{\int_{-\infty}^{\infty} J''(\omega) d \ln(\omega)}{(J_R - J_U)} = \int_{-\infty}^{\infty} \psi''(\omega) d \ln(\omega) = \frac{\pi}{2} \quad (5)$$

The intrinsic difficulty with modelling relaxation behaviour is that it is not generally possible, knowing the shape of the relaxation in time or frequency, to work backwards to determine $\phi(\ln \tau)$. The problem is often referred to as mathematically ‘ill conditioned’. One solution would be to examine candidate forms for $\phi(\ln \tau)$, and determine by trial and error, using equations (2)–(4) the most form appropriate to fit the relaxation in question. This entails numerical integration since such functions are not generally amenable to analytical integration. There are, however, two models, C–C and Havriliak–Negami (H–N)^{4–6} that provide analytical expressions for both the retardation time distribution and the viscoelastic parameters, J' and J'' . These form the basis of the present study.

Cole–Cole model^{4,5}

This offers relatively simple analytical expressions for the compliance functions and for the retardation time distribution. The broadening of the retardation spectrum is characterised by modifying the complex term in the Debye expression for J^* by adding a ‘broadening’ factor α , so that



5 Retardation time distributions, corresponding to $\alpha=0.8, 0.4$ and 0.2 , from C-C distribution, equation (7)

$$J^*(\omega) = J_U + (J_R - J_U) \frac{1}{1 + (i\omega\tau_0)^\alpha} \tag{6}$$

where $0 < \alpha < 1$, with $\alpha=1$ corresponding to the SRT model. Lower α values correspond to broader, but SRT spectra. Equation (6) corresponds to the following retardation time distribution function

$$\phi(\ln \tau) = \frac{1}{2\pi} \frac{\sin(\alpha\pi)}{\{\cosh[\alpha \ln(\tau/\tau_0)] + \cos(\alpha\pi)\}} \tag{7}$$

which characterises a range of symmetrical distribution functions, examples of which are shown in Fig. 5. Here, τ_0 is the time corresponding to the maximum in the retardation time distribution. Applying de Moivre's theorem to equation (6) gives expressions for the storage and loss compliances

$$J'(\omega) = J_U - (J_R - J_U) \frac{1 + (\omega\tau_0)^\alpha \cos(\pi\alpha/2)}{1 + 2(\omega\tau_0)^\alpha \cos(\pi\alpha/2) + (\omega\tau_0)^{2\alpha}} \tag{8}$$

and

$$J''(\omega) = (J_R - J_U) \frac{(\omega\tau_0)^\alpha \sin(\pi\alpha/2)}{1 + 2(\omega\tau_0)^\alpha \cos(\pi\alpha/2) + (\omega\tau_0)^{2\alpha}} \tag{9}$$

The C-C model thus gives

$$\psi'(\omega) = \frac{1 + (\omega\tau_0)^\alpha \cos(\pi\alpha/2)}{1 + 2(\omega\tau_0)^\alpha \cos(\pi\alpha/2) + (\omega\tau_0)^{2\alpha}}$$

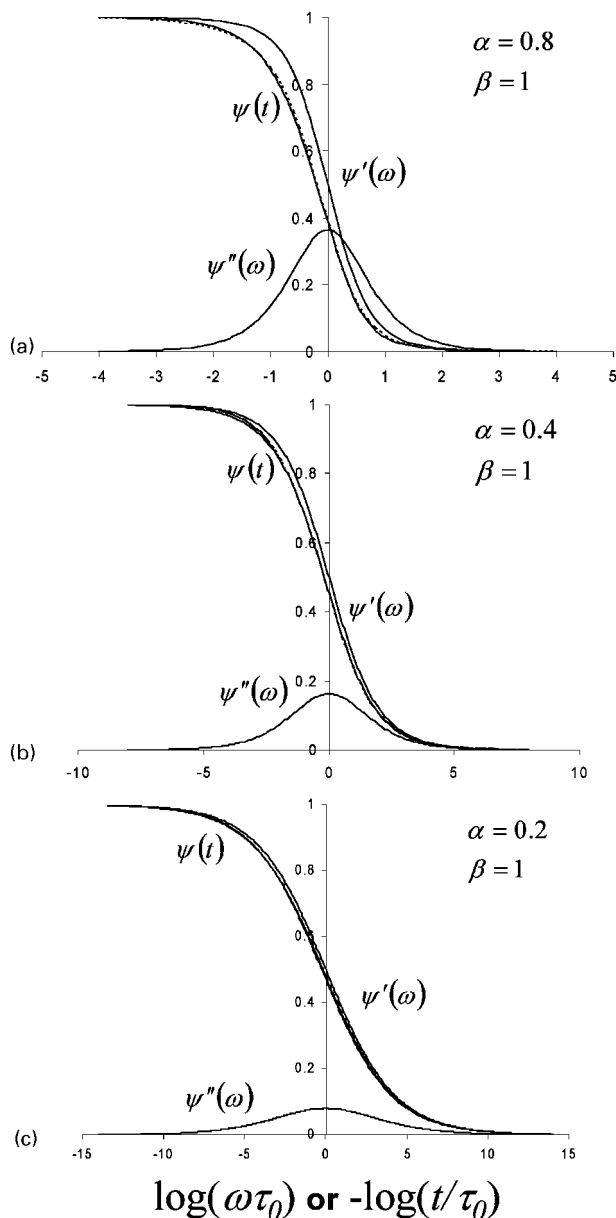
and

$$\psi''(\omega) = \frac{(\omega\tau_0)^\alpha \sin(\pi\alpha/2)}{1 + 2(\omega\tau_0)^\alpha \cos(\pi\alpha/2) + (\omega\tau_0)^{2\alpha}}$$

Figure 6 shows some examples of $\psi'(\omega)$, $\psi''(\omega)$ and $\psi(t)$ for the C-C model with different values of α .

There is no analytical expression for $\psi(t)$. Apart from the SRT model all other models require numerical integration to evaluate the creep function. Equation (4) was integrated numerically to give the data in Fig. 6c.

It can be seen that $\psi'(\omega)$ and $\psi''(\omega)$ show antisymmetrical and symmetrical behaviour respectively, when plotted against log frequency. By contrast, the creep function, $\psi(t)$, shows lack of symmetry when plotted against log time. This is most pronounced at high α values. For broader retardation time spectra (i.e. lower α values) the curves for $\psi(t)$ become more regular in shape and antisymmetrical, such as the curves for $\psi'(\omega)$,



6 Compliance functions, $\psi'(\omega)$, $\psi''(\omega)$ and $\psi(t)$ calculated from C-C model, for α values of a 0.8, b 0.4 and c 0.2: approximation for $\psi(t)$, equation (10) is shown as dotted line in each case

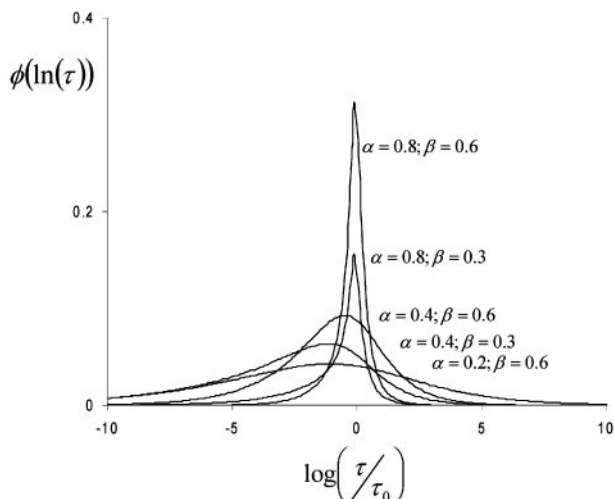
eventually beginning to resemble the $\psi'(\omega)$ curves. Some use may be made of this effect in the modelling of creep behaviour. Noting that $\psi(t) = 1 - \psi'(\omega)$ in the fully relaxed and unrelaxed cases, it was found that $\psi(t)$ could be estimated to sufficient accuracy by assuming it to be a power law function of $1 - \psi(t)$, using the same numerical values for ω and τ , i.e.

$$\psi(t) = \left[1 - \psi'(\omega)_{\omega\tau_0 = \frac{t}{\tau_0}} \right]^m$$

so

$$\psi(t) = \left[\frac{(t/\tau_0)^\alpha \cos(\pi\alpha/2) + (t/\tau_0)^{2\alpha}}{1 + 2(t/\tau_0)^\alpha \cos(\pi\alpha/2) + (t/\tau_0)^{2\alpha}} \right]^m \tag{10}$$

The predicted values of $\psi(t)$ were matched to the ones obtained by numerical integration by varying the value of m to achieve the best least squares fit between the



7 Retardation time distributions from asymmetrical H–N distribution, equation (31) for various values of α and β : key – in order of decreasing peak height $\alpha=0.8, \beta=0.6$; $\alpha=0.8, \beta=0.3$; $\alpha=0.4, \beta=0.6$; $\alpha=0.4, \beta=0.3$; $\alpha=0.2, \beta=0.6$

functions over the full relaxation range for each α value. It was found that m could be related to α by

$$m = 1 - 0.2546\alpha - 0.1568\alpha^2 \tag{11}$$

As α approaches zero, m approaches 1. Indeed, for many of the engineering polymers and composites of greatest interest the T_g relaxation may be broad enough to make the approximation that $m=1$. In other words the creep modulus for time t is numerically equivalent to the DMTA modulus for a frequency of $1/t$. This near equivalence between DMTA and creep data could be of considerable practical value in estimating creep behaviour of polymers and composites from DMTA data.

Applying equation (5) to the C–C model it can be further shown that

$$\frac{J''(\omega)_{\max}}{(J_R - J_U)} = \psi''(\omega)_{\max} = \frac{1}{2} \tan\left(\frac{\alpha\pi}{4}\right) \tag{12}$$

so

$$\alpha = \frac{4}{\pi} \arctan\left[\frac{2J''(\omega)_{\max}}{(J_R - J_U)}\right] = \frac{4}{\pi} \arctan[2\psi''(\omega)_{\max}] \tag{13}$$

When DMTA data are available, α can be found directly from the maximum value of J'' . The C–C model therefore offers a framework in which to describe time dependent isothermal behaviour using simple expressions, provided the material can be shown to have a symmetrical retardation time distribution.

Havriliak–Negami model^{6,7}

This uses a further parameter β to describe the asymmetry of the retardation time distribution. In this case the Debye equation is further modified from the form of equation (6) to

$$J(\omega) = J_U - \frac{J_R - J_U}{[1 + (i\omega\tau)^\alpha]^\beta} \tag{14}$$

For $\beta=1$ the H–N model reduces to the C–C model. Usually $0 < \beta < 1$, although values greater than 1 are also possible. The H–N retardation time distribution is

$$\phi(\ln \tau) =$$

$$\frac{1}{\pi} \left(\frac{\tau}{\tau_0}\right)^{\alpha\beta} \sin\left\langle \beta \arctan\left\{ \frac{\sin(\pi\alpha)}{\left[\left(\frac{\tau}{\tau_0}\right)^\alpha + \cos(\pi\alpha)\right]} \right\} \right\rangle / \left[\left(\frac{\tau}{\tau_0}\right)^{2\alpha} + \left(\frac{\tau}{\tau_0}\right)^\alpha \cos(\alpha\pi) + 1 \right]^{\beta/2}$$

Examples of this distribution are shown in Fig. 7. The corresponding relaxation functions for the H–N model are

$$\psi' =$$

$$\cos\left\langle -\beta \arctan\left\{ (\omega\tau)^\alpha \sin\left(\frac{\pi\alpha}{2}\right) / \left[1 + (\omega\tau)^\alpha \cos\left(\frac{\pi\alpha}{2}\right)\right] \right\} \right\rangle / \left[1 + (\omega\tau)^{2\alpha} + 2(\omega\tau)^\alpha \cos\left(\frac{\pi\alpha}{2}\right)\right]^{\beta/2}$$

and

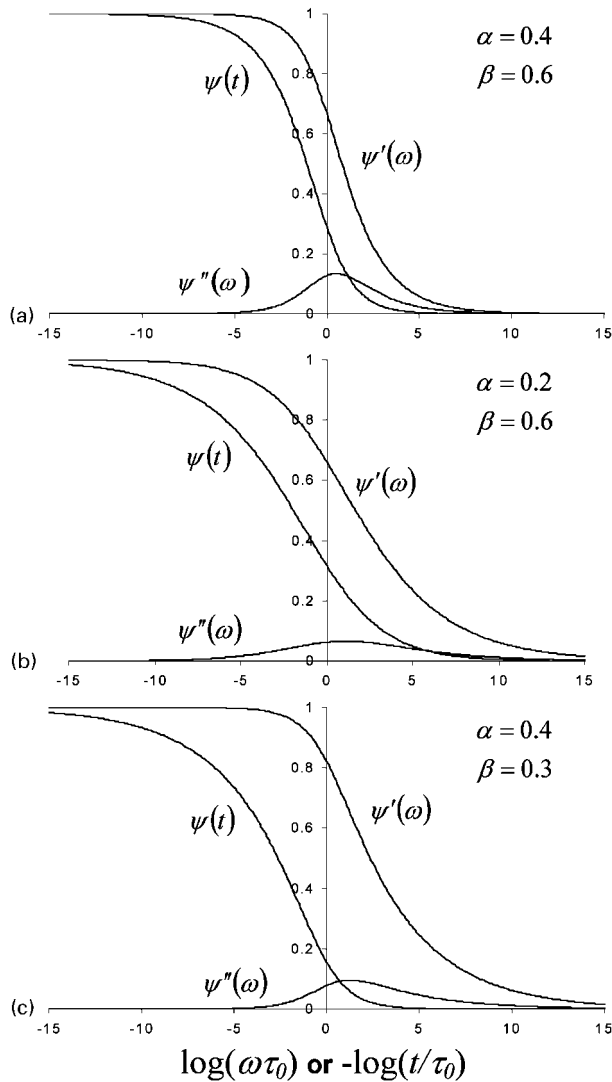
$$\psi'' =$$

$$\sin\left\langle -\beta \arctan\left\{ (\omega\tau)^\alpha \sin\left(\frac{\pi\alpha}{2}\right) / \left[1 + (\omega\tau)^\alpha \cos\left(\frac{\pi\alpha}{2}\right)\right] \right\} \right\rangle / \left[1 + (\omega\tau)^{2\alpha} + 2(\omega\tau)^\alpha \cos\left(\frac{\pi\alpha}{2}\right)\right]^{\beta/2}$$

Figure 8 shows some examples of $\psi'(\omega)$, $\psi''(\omega)$ and $\psi(t)$, plotted against log frequency or log time, for the H–N model with different values of α and β . The effects of the skewness of the retardation time distribution can be seen to be reflected in these curves. Unfortunately with this type of distribution there is no longer any convergence of creep function and storage function in the case of broad distributions, so approximations of the type discussed for the C–C model are not possible. It can also be seen that the skewed nature of the distribution results in shifts along the log time or frequency axes, so the peak of the distribution no longer corresponds to the origin of the horizontal axis.

Cole–Cole plot

This is a plot of J'' versus J' or, as here, in non-dimensional form, ψ'' versus ψ' . The C–C plot forms an arc, the shape of which is characteristic of the type of retardation time distribution for the material and the relaxation. For $\alpha=\beta=1$, the SRT model, for instance, the C–C plot forms a semicircular arc. For the symmetrical C–C distribution a family of flattened symmetrical arcs is obtained, while for the H–N model the arcs are skewed. Figure 9 shows C–C plots for all the DMTA results discussed here. Given the different types of reinforcement architecture these arcs are very similar in the present case. They are also symmetrical, suggesting, in the present case at least that the C–C model may be applied, rather than the more complex H–N model. This provided an opportunity to investigate the approximate model, based on C–C, for predicting creep behaviour from DMTA. The C–C plot can be seen to be extremely powerful as an aid to characterising the shape of the retardation time distribution, regardless of any temperature dependence, which has yet to be discussed. It should be noted that the results in Fig. 9 relate to a broad range of temperatures. The model curves, the continuous lines in this figure were not obtained by varying α to achieve the best fit. The values of α were simply obtained by inserting the maximum value of ψ'' into equation (13).



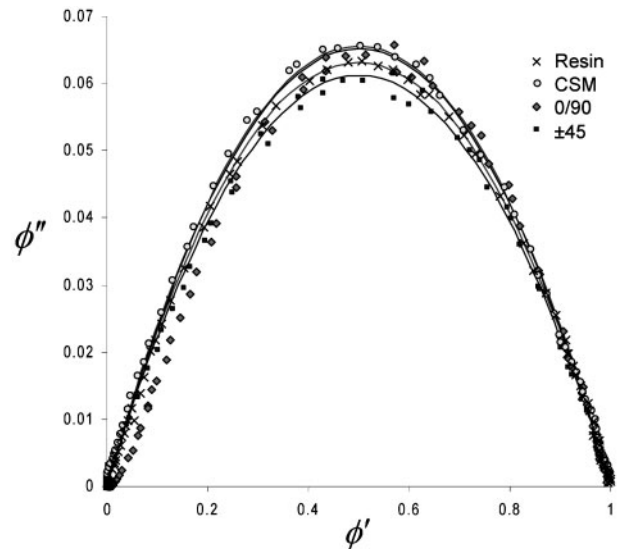
8 Compliance functions, $\psi(\omega)$, $\psi''(\omega)$ and $\psi(t)$ calculated from H-N model, for a $\alpha=0.4$, $\beta=0.6$, b $\alpha=0.2$, $\beta=0.6$ and c $\alpha=0.4$, $\beta=0.3$

Behaviour as function of temperature

For modelling DMTA curves in varying temperature it is necessary to relate changes in frequency or time to changes in temperature. Assuming the characteristics of a relaxation process not to change over a range of temperatures and frequencies is generally known as treating the material as 'rheologically simple'. In some cases, and for particular relaxations, contour plots over the time/temperature domain show the material not to follow this behaviour. However, for the T_g of thermosetting resin systems such as the polyester considered here, the assumption appears to be justifiable. In the present work, Arrhenius dependence of the relaxation time was assumed (with constant activation energy for all the retardation times) purely because this produces a linear equivalence between the log time (or frequency) and $1/T$. Using Arrhenius, the temperature dependence of τ is given by

$$\tau = \tau_0 \exp\left(\frac{H}{RT}\right) \tag{15}$$

A change in temperature can be regarded as equivalent to a shift in time or frequency. If T_0 is the temperature at which the peak of the relaxation time spectrum has some reference value (say, 1 s), it is possible to define a shift



9 Cole-Cole plots for DMTA experimental data: pure resin ($\alpha=0.160$); CSM composite ($\alpha=0.166$); 0/90° composite ($\alpha=0.155$), and $\pm 45^\circ$ composite ($\alpha=0.165$)

factor, and the logarithmic shift in relaxation time is

$$\ln(a_T) = \ln\left(\frac{\tau}{\tau_0}\right) = \frac{H}{R} \left(\frac{1}{T_0} - \frac{1}{T_R}\right) \tag{16}$$

It is possible, simply to add the shift factor to each term in $\ln(\omega\tau_0)$ or $\ln(t/\tau_0)$. Some simplification can be achieved when it is formally assumed that T_0 is the temperature at which $\ln(\omega\tau_0) = 1$ at 1 Hz or $\ln(t/\tau_0) = 1$ at 1 s, depending on whether DMTA or creep is being modelled. These terms reduce to

$$\begin{aligned} \ln(\omega\tau_0) &= \ln(\omega) + \frac{H}{R} \left(\frac{1}{T_0} - \frac{1}{T_R}\right) \\ \ln(t/\tau_0) &= \ln(t) + \frac{H}{R} \left(\frac{1}{T_0} - \frac{1}{T_R}\right) \end{aligned} \tag{17}$$

Modelling the behaviour in the temperature plane rather than in frequency simply involves substituting the $\omega\tau$ term in the C-C or H-N models by the above expression.

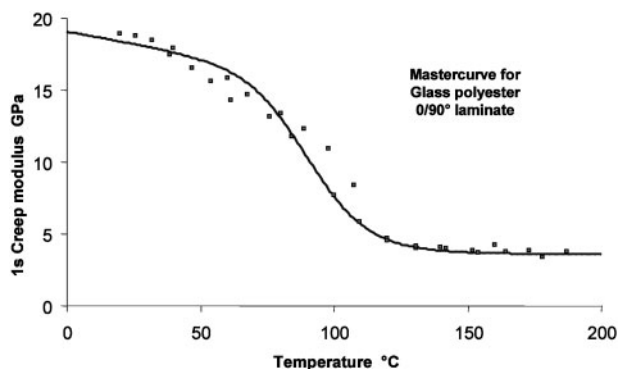
In modelling behaviour as a function of temperature it is often necessary to take account of the temperature dependence of the relaxed and unrelaxed values of the moduli or compliances¹⁻³. In the present case it will be considered that the unrelaxed modulus is linearly dependent on temperature, so

$$E_U = E_{U_0} - kT' \tag{18}$$

In summary, the model examined here required seven constants to fully fit a set of thermomechanical data, these being: α , β , E_U , E_R , k , T_R and H . The number of constants could be reduced, for instance when the C-C model applies, rather than the H-N, so $\beta=1$, or if the temperature dependence of E_U could be neglected. Alternatively, an additional constant would be needed if the temperature dependence of E_R were taken into account, which might be required if improved accuracy was required in the high temperature region.

Results and discussion

As mentioned earlier, all four sets of results give symmetrical C-C plots, implying that the retardation



10 Flexural creep modulus in 0° direction versus temperature for glass/polyester 0/90° laminate. Master curve, shifted to 1 s, for the data shown in Fig. 3, fitted using the parameters from Table 1

time distribution is symmetrical in log retardation time space. In the present case at least, therefore, the results can be fitted by the C–C model, rather than the more general H–N model, so it will be assumed that $\beta=1$.

The theoretical treatment discussed here is set out mainly in terms of compliances rather than moduli. However, most engineers and scientists are more familiar with the latter. Therefore, the results and modelling in Figs. 1, 2, 3 and 10 have been expressed in terms of moduli, obtained from the compliances using the well known reciprocal relationships.

The data points in Figs. 1 and 2 were fitted with continuous curves from the C–C model, using the parameters shown in Table 1. The α values were obtained directly from the maximum loss compliance values and the relaxed and unrelaxed compliances, using equation (13). As mentioned already, E_U and E_R were obtained from the flexural creep measurements. The C–C plot is of great value in enabling the general form of the retardation time distribution to be obtained and checked, even when the results are non-isothermal – the only temperature – dependent parameter being the minor temperature dependence parameter k .

The remaining major parameters T_R and H could possibly have been determined by trial and error, minimising the least square error between the measured and predicted data. However, their effect on the predicted spectra is rather similar, so this method has not resulted in an accurate determination. Instead, an estimate was made of the activation energy H using time temperature superposition of the creep data at different times, using equation (16). This resulted in a value of H/R of 34 000 K. This value was close to values obtained in previous work on polyester resins, so this value was assumed in modelling all the data. In hindsight, a more accurate method of determining the activation energy may have been to measure the DMTA data over a range of frequencies, but this was not envisaged at the outset of the work.

The two remaining parameters T_R and k were then obtained for each laminate type, by varying them to achieve a minimum least squares deviation between the measured and modelled moduli and loss moduli, giving equal weight to each parameter. The final values of the parameters used to fit the curves are shown in Table 1.

Figures 1 and 2 generally show a good agreement between measured and modelled parameters. The agreement is especially good in the case of the storage

moduli, which are probably the main parameters of interest. Agreement with the loss moduli was fairly good, although there appears to be a consistent problem with modelling the low temperature side of the relaxation peaks. Nevertheless, even here, the agreement was acceptable and would certainly be good enough for characterising and interpreting data in terms of the C–C model. The reason for the loss modulus discrepancy is not known. One possibility could be post-curing of the resin during the DMTA run. However, significant efforts were made to avoid such a problem by subjecting the laminates to a rigorous post-curing schedule before testing. This minor difficulty could be a subject of the future study. The fact that most of the data lie so close to the C–C model line is very encouraging and could certainly form a basis for the future modelling of temperature dependent behaviour.

The value of m to be used in the creep modelling was found from equation (11) to be 0.96. This was used along with equations (10) and (4) to obtain the curve for the 1 s creep modulus, shown as the master curve in Fig. 9. The difference between this and the curve for $m=1$ would have been negligible. The agreement with the creep data is also encouraging, although the overall scatter of the creep data is rather larger than that for the DMTA data.

Conclusions

This investigation identified the C–C model and the H–N model, respectively as suitable bases for the modelling of time and temperature behaviour of composites with symmetrical and asymmetrical retardation time spectra.

In the case of the C–C model an approximate shortcut method was identified for the prediction of creep behaviour from DMTA data.

The resin and composites examined in this study all showed symmetrical retardation time spectra and their DMTA behaviour was well modelled using the C–C model with the added assumption of Arrhenius kinetics for the relaxation. The proposed creep model also worked well for these materials.

Acknowledgements

Some of the mechanical property data employed in the present paper were generated by Dr T. N. A. Browne for use in a PhD project on the fire behaviour of composite structures under load. The present paper was presented at the International Conference on Structural Analysis of Advanced Materials (ICSAM-07), Patras, Greece, 2–5 September, 2007.

References

1. N. G. McCrum, B. E. Read and G. Williams: 'Anelastic and dielectric effects in polymeric solids'; 1991, New York, Dover.
2. J. D. Ferry: 'Viscoelastic properties of polymers', 3rd edn; 1980, New York, John Wiley and Sons.
3. I. M. Ward: 'Mechanical properties of solid polymers', 2nd edn; 1983, New York, John Wiley.
4. R. H. Cole and K. S. Cole: *J. Chem. Phys.*, 1941, **9**, 341.
5. R. H. Cole and K. S. Cole: *J. Chem. Phys.*, 1942, **10**, 98.
6. S. Havriliak and S. Negami: *Polymer*, 1967, **8**, (4), 161–210.
7. S. Havriliak and S. J. Havriliak: 'Dielectric and mechanical relaxation in materials'; 1997, Munich, Hanser.